AN INVESTIGATION INTO WING IN GROUND EFFECT AIRFOIL GEOMETRY

N.Moore, Professor P A.Wilson, A J.Peters (*)
School of Engineering Sciences, University of Southampton, SO17 1BJ, UK
(*) QinetiQ Haslar

Nomenclature

AoA	Angle of Attack
AR	Aspect Ratio
b	Wing span
c	Wing chord
C_D	Drag coefficient, $D/½\rho v^2 S$
C_L	Lift coefficient, $L/½\rho v^2 S$
C_m	Pitching moment coefficient, $M/½\rho v^2 Sc$
C_P	Pressure coefficient
CFD	Computational Fluid Dynamics
DHMTU	Department of Hydro-mechanics of the Marine Technical University
D	Drag force
FSU	Former Soviet Union
h/c	Height to chord ratio
IGE	In Ground Effect
L	Lift force
L/D	Lift to Drag ratio
M	Pitching moment
NACA	National Advisory Committee on Aeronautics
OGE	Out of Ground Effect
Re	Reynolds number based on chord
S	Wing area
V	Free stream speed
WIG	Wing In Ground Effect
α	Angle of attack

Summary

This paper details experimental results from wind tunnel studies of a DHMTU 12-35.3-10.2-80.12 and NACA 0012 section operating in ground effect. It was found that the drag of the DHMTU 12-35.3-10.2-80.12 increased with decreasing altitude, contrary to expectations and superior lift performance to the NACA 0012 baseline section was generated. The DHMTU possesses superior L/D at low angles of attack when in ground effect. These experimental studies have illustrated the unique aerodynamic characteristics of the DHMTU 12-35.3-10.2-80.12 and indicated areas for further optimisation of the design of ground effect airfoils.

Introduction

Wing In Ground (WIG) effect craft are unique vehicles that operate at altitudes of several metres above the sea surface to take advantage of favourable aerodynamic interactions between the wing and ground. Previous studies have found that with decreasing altitude a rapid increase in lift and a

reduction in vortex drag is produced. This results in the Lift to Drag (L/D) ratio, also known as the aerodynamic efficiency, of the wing increasing. Thus flying In Ground Effect (IGE) potentially offers a very economical form of rapid transport.

Ground effect can be divided up into two distinct regimes, ram and normal ground effect [1]. Ram ground effect occurs where the wing is at an altitude of h/c=0.1 or less. Here the wing is so close to the ground that the trailing edge of the wing is creating a sealed envelope. The airfoil is operating on a trapped cushion of air, using the same principal as a hovercraft. As the airfoil's altitude increases, it enters what is normally considered to be normal ground effect. This regime extends from just above the "ram wing" height (h/c>0.1) to approximately half the wings span off the ground.

WIG craft have been have been proposed for heavy lift, Special Forces insertion, maritime strike, anti-submarine warfare and amphibious assault missions. Operational advantages possessed by WIGs are:

- Rapid dispersion from vulnerable bases during times of hostility
- Rapid ingress and egress capability
- Reduced detection range compared to aircraft, WIG craft would only be flying at an altitude of several metres resulting in the defender possessing a limited radar horizon, typically 20-40 km.
- Speed advantage over conventional sea borne vessels, several hundred knots for a WIG compared to tens of knots for hydrofoils and other surface borne craft.
- WIGs are invulnerable to torpedoes and mines
- WIG's posses a very low acoustic signature [2]

Over the past two decades several military WIG concepts have been proposed in the West but none have been constructed [3, 4]. This in contrast with the Former Soviet Union (FSU) who is acknowledged as having taken the lead in military WIG research and development. The FSU developed and flight tested transport (ORLYONOK) and maritime strike (LUN) WIGs.

Two of the key issues that need to be addressed to realise the full operational capability of these vehicles are dedicated ground effect wing airfoil design and the resulting performance over the dynamic sea surface.

In order to assess the applicability of an airfoil section for operation IGE, performance requirements need to be formulated. Table 1 presents 3 metrics that a WIG airfoil must posses:

- Aerodynamic efficiency
- Stability
- Controllability

A high L/D figure for a range of operational altitudes is required to provide for economical operation. Minimum change in pitching moment with variation in height produces a stable section. To aid in WIG controllability a gradual change in lift with altitude is required.

Requirement	Expression	Comment
High L/D at cruising altitudes	$\frac{C_L}{C_D} = \text{maximum}$	Maximum possible efficiency when operating IGE
Stability	$\frac{C_m}{C_L}(h) = \text{minimum}$	Minimum movement of Aerodynamic Centre with variation in height
Controllability	$\frac{\partial C_L}{\partial H} = \text{minimum}$	Gradual change of handling characteristics in operating regime

Table 1: WIG Airfoil Requirements

In an operational environment a WIG will be transiting over the sea, the oscillatory nature of this dynamic surface places additional requirements on the section. The variations in lift, pitch and drag in response to the dynamic surface have to be investigated. These cyclic changes make demands on the control system and may produce structural fatigue and disorientation of personnel on board the WIG. This particular aspect of the wing IGE is presently being addressed in the research.

At present very little information on practical dedicated ground effect airfoils and their operation in a maritime environment has been published in open literature. In the West conventional airfoil series have been utilised in WIG studies and prototype testing. The FSU developed a dedicated family of airfoil sections known as the DHMTU (Department of Hydro-mechanics of the Marine Technical University) series, though little detailed information on the performance of these sections has been published.

Research Philosophy and Aims

The research at the University of Southampton is concerned with investigating and understanding the relationship between section geometry and performance of dedicated ground effect wing sections operating in a realistic marine environment. This paper details initial experimental investigations into the first iteration of a dedicated ground effect section.

It was decided early on in the research program to initially adopt an experimental approach. This decision was based upon:

- the lack of any sufficiently detailed database on dedicated airfoil sections operating IGE.
- a desire to obtain some 'real' indigenous data and gain a first hand appreciation of ground effect physics.
- theoretical and computational research methods require some form of empirical data for validation at some stage of their development.

Methodology

The methodology selected has been to obtain experimental data and behaviour for a range of sections in wind tunnels and towing tanks. This will form the basis of numerical optimisation and CFD studies that are to be carried out in the near future.

The approach taken has been to reverse engineer a Russian DHMTU section to investigate the performance and design characteristics of this family. During the initial stages of the research very little was known about the characteristics of practical dedicated ground effect sections. The

choices made in deciding the DHMTU section geometry was based upon minimal experience with the DHMTU family.

DHMTU sections are characterised by a flat undersurface and an S-shaped mean line. A DHMTU section is described by 8 numbers, which define the geometry of the upper and lower surfaces. The format being DHMTU a-b.c-d.e-f.g.h, the section tested is a DHMTU 12-35.3-10.2-80.12.2, for reasons of brevity it is known throughout this paper as DHMTU. Tables 2 and 3 lists the parameters and values used for the test section. Figure 1 illustrates a section through the DHMTU 12-35.3-10.2-80.12.2.

The geometry of the profile used was based upon information gleaned from a South Korean website [6] and iterations in XFOIL [7]. The DHMTU section was given a t/c ratio of 12% because this was the value of the NACA control section.

Prefix	Definition	Experimental Value
a	maximum ordinate of the upper surface (%c)	12
b	position of the maximum ordinate (%c)	35
c	ordinate of the start of the flat section (%c, below the horizontal is positive)	3
d	position of the start of the flat section (%c)	10
e	ordinate of the end of the flat section (%c, below the horizontal is positive)	2
f	position of the end of the flat section (%c)	80
g	slope parameter of the upper trailing edge	12
h	nose radius parameter	2

Table 2: DHMTU Properties

Figure 1: DHMTU 12-35.3-10.2-80.12.2 Profile

To provide a baseline section for comparison with the DHMTU a symmetrical NACA 0012 airfoil section was used (Figure 2). This was selected as it provides conventional aerodynamic performance to act as a datum for the sections studied in this research.


Figure 2: NACA0012 baseline section

	NACA 0012	**DHMTU 12-35.3-10.2-80.12.2**
Span	0.96 m	0.96 m
Aspect Ratio	3.02	3.01
t/c	12%	12%
Chord	0.317 m	0.319 m
Area	0.303 m2	0.306 m2
Wing Sweep	0 degrees	0 degrees

Table 3: DHMTU and NACA 0012 Parameters

The measurements were taken in Southampton Universities 2.1 x 1.7 m rolling road wind tunnel. The wind tunnel is open at both ends and is located in a large building, which serves both as an inlet plenum and a discharge chamber. The flow is driven by six 3 m rotating fans and regulated by controlling the speed of the DC motors that drive the fans. The maximum airflow and road speed produced by the tunnel is 40 ms^{-1} in the working section. A rear view of the model, sting and moving road is shown in Figure 3.


Figure 3: DMTU section in 2.1 x 1.7 m rolling road wind tunnel

All the wind tunnel runs were conducted at a free stream velocity of 38 ms^{-1} unless otherwise stated. This corresponds to a Reynolds's Number of 8 x 10^5 based upon wing chord. To simulate the actual flow conditions encountered when a wing flies close to the ground the road surface was run at 38 ms^{-1}. The sections were tested at angles of attack ranging from –5 to +13 degrees, with readings being taken at every 1 degree step. The section was tested at a height of h/c=2.3 which is considered to be operating OGE and between h/c 1.0 to 0.08. The variables for the experiments are summarised in Table 4. Tare and blockage corrections have been taken into account and included in the analysis.

Variable	Range
Angle of Attack	-5 to 13 degrees (1 degree steps)
Wing Height (h/c)*	2.3, 1.0 to 0.1 (0.1 steps) and 0.08
Reynolds's Number	8×10^5, 4×10^5, 1×10^5

Table 4: Test Variables

*Wing height was measured at c/3

Discussion of Results

The overall drag of the DHMTU section reduces with decreasing altitude, as illustrated in Figure 4. This is an interesting feature of the DHMTU, as total drag usually increases due to the increase in pressure drag with decreasing altitude. This can be seen in Figure 5 which depicts the drag performance of the NACA 0012 section showing the increase in drag with decreasing altitude.

The continued reduction in drag for the DHMTU section may be due to the dominance of vortex drag in the overall drag of the section. As is well documented the vortex drag reduces with a decrease in altitude [1]. This may account for the behaviour seen in Figure 4. Once the section reaches h/c=0.6 or lower the reduction in drag does not become significant with decreasing altitude.

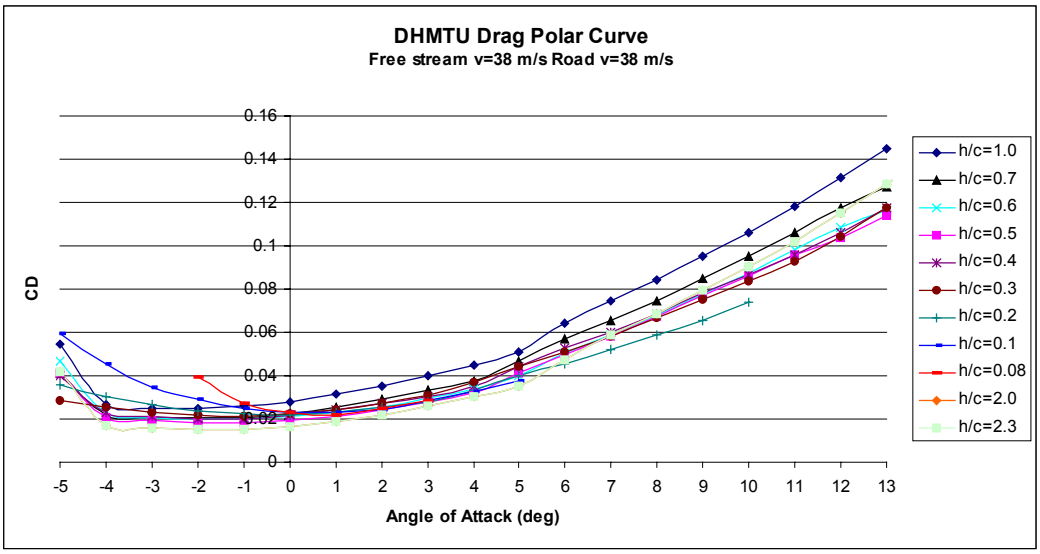

Figure 4: DHMTU Drag Polar

Comparisons of the NACA 0012 and DHMTU drag polars (Figure 5) shows that at h/c=0.3 the DHMTU section produces 2 to 2.9 times the amount of drag of the NACA 0012. As the altitude decreases to h/c=0.2 the DHMTU section produces 1.6 to 1.8 the drag of the NACA. A further decrease in altitude to h/c=0.1 reveals that the DHMTU is producing 1.3 to 1.6 of the drag of the NACA 0012. An exception to this is when the AoA falls below 1 degree where due to blockage the NACA 0012 produces more drag. In normal ground effect the DHMTU section produces 1.3 to 2.9 times the amount of drag of the NACA 0012 at altitudes between h/c=0.3 to 0.1 (Table 5).

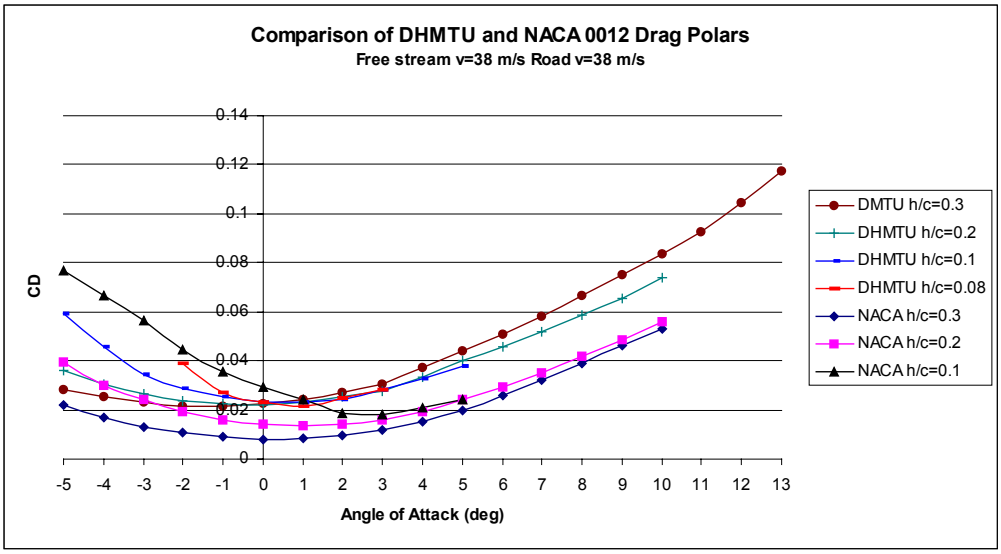

Figure 5: Comparison of DHMTU and NACA 0012 Drag Polars

H/c	DHMTU C_D	NACA 0012 C_D	NACA C_D/DHMTU C_D
1	0.050696	0.022255	2.3
0.9	0.046829	0.024358	1.9
0.8	0.04887	0.020171	2.4
0.7	0.046919	0.016517	2.8
0.6	0.040088	0.021928	1.8
0.5	0.041337	0.022808	1.8
0.4	0.044152	0.022887	1.9
0.3	0.044088	0.019853	2.2
0.2	0.039809	0.024066	1.7
0.1	0.037813	0.024301	1.6

Table 5: Comparison of DHMTU and NACA 0012 Drag Magnitudes as a function of altitude

The reduction in Reynolds Number produces an increase in the drag characteristics of the DHMTU (Figure 6). It can be seen that at Re=1 x 10^5 at AoA greater then 1 degree the drag increases significantly. This is indicative of the boundary layer exhibiting laminar flow but separating at an earlier point then at the higher Reynolds Number cases. There is very little difference between the drag values when the moving ground surface is turned off. Values of drag with the ground turned off vary only by a maximum of 0.6% with road on drag values.

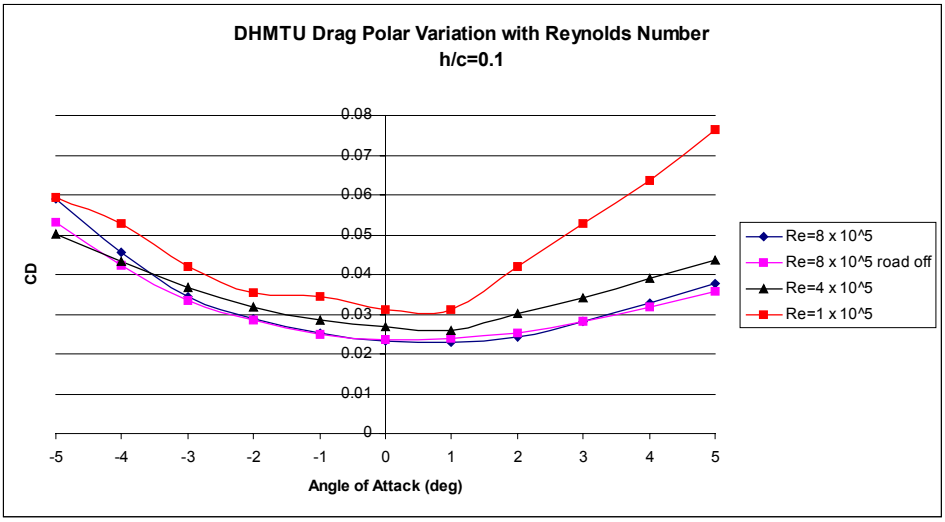

Figure 6: Effect of Reynolds Number variation on DHMTU drag characteristics

It was mentioned in the Introduction that the lift of a section increases as the proximity to the ground decreases. As well as conforming to this trend the DHMTU section also exhibits other interesting features. A step change in the lift curve gradient is exhibited at all altitudes, this can be seen in Figure 7. As the h/c decreases the angle of attack at which this step occurs reduces (Table 6). When the section is at h/c=1 the step occurs at an angle of attack of 5 degrees reducing to 1 degree AoA for h/c=0.08.

Though the data did not extend up to the stall angle of the section, due to constraints in the mounting apparatus, Figure 7 provides indications that the stall angle is reducing as altitude decreases. At h/c=0.5 maximum C_L is obtained at 12 degrees AoA, by implication the stall angles for greater h/c were not seen as they occurred at higher angles of attack. Stall behaviour was not observed at lower altitudes due to the ground clearance constraint on AoA.

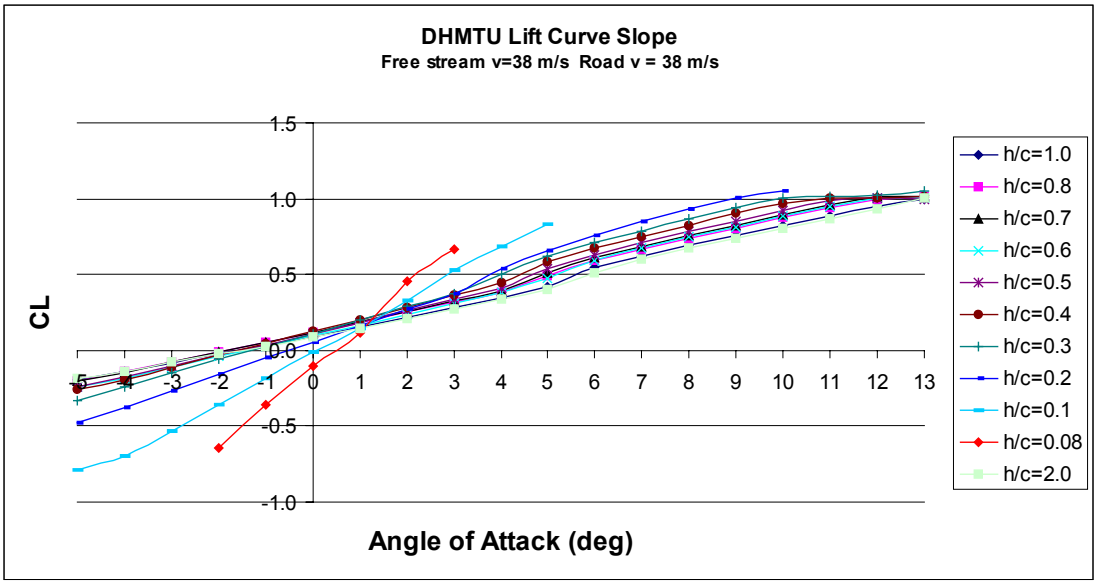

Figure 7: DHMTU Lift Curve Slope

As the section approaches the ground the lift curve slope gradient ($dC_L/d\alpha$) increases (Table 6). At h/c=1 values of $dC_L/d\alpha$ in the range 3.5 radian^{-1} to 3.7 radian^{-1} are obtained, as the section reaches extreme ground effect this increases to 12 radian^{-1} to 14.5 radian^{-1}. This can be compared to the lift curve slope gradient of the NACA 0012 that possesses similar values except in extreme ground effect.

h/c	Step (deg)	Pre-step $dC_L/d\alpha$ (units of lift per radian)	Post-step $dC_L/d\alpha$ (units of lift per radian)
1.0	5	3.5	3.7
0.9	5	3.7	3.7
0.8	4	3.7	3.8
0.7	4	3.8	3.8
0.5	4	4.1	4.0
0.4	4	4.5	3.8
0.3	3	5.0	4.4
0.1	2	12.0	N/O
0.08	1	14.5	N/O

Table 6: DHMTU Lift Curve Slope Gradient for various Altitudes

N/O Not Obtainable

Altitude (h/c)	$\frac{dC_L}{d\alpha}$ per radian
1	3.7
0.9	3.7
0.8	3.9
0.7	4.0
0.6	4.2
0.5	4.2
0.4	4.8
0.3	5.2
0.2	6.9
0.15	8.8
0.1	9.3

Table 7: NACA 0012 Lift Curve Slope Gradient as a function of altitude

Figure 8 illustrates the comparison in lift performance of the NACA 0012 and DHMTU sections between h/c=0.3 to 0.1. The DHMTU section has superior lift characteristics between altitudes of h/c=0.1 to 1. An interesting observation is that when the NACA 0012 is at h/c=0.1 large downward forces are produced when AoA reduces below 3 degrees. These large downward coefficients are probably a result of the suction effect caused by the lower surface and the flat ground surface. These suction forces can be seen to be present at h/c 0.2 and 0.3 but they are less dominant. The superior performance of the DHMTU IGE can be ascribed to the favourable interaction between the geometry of the lower section and ground. This illustrates the importance of optimally designing the lower surface of the section for operation IGE.

Table 8 illustrates the superior lifting producing capability of the DHMTU over the NACA 0012 at an AoA of 5 degrees. It can be seen that the DHMTU generates between 1.4 to 2.1 times the lift of the NACA 0012 when operating IGE.

H/c	DHMTU C_L/NACA 0012 C_L
1	1.5
0.9	1.4
0.8	2.0
0.7	2.1
0.6	1.6
0.5	1.7
0.4	1.8
0.3	1.7
0.2	1.6
0.1	1.6

Table 8: Ratio of DHMTU CL/NACA CL at AoA 5 degrees

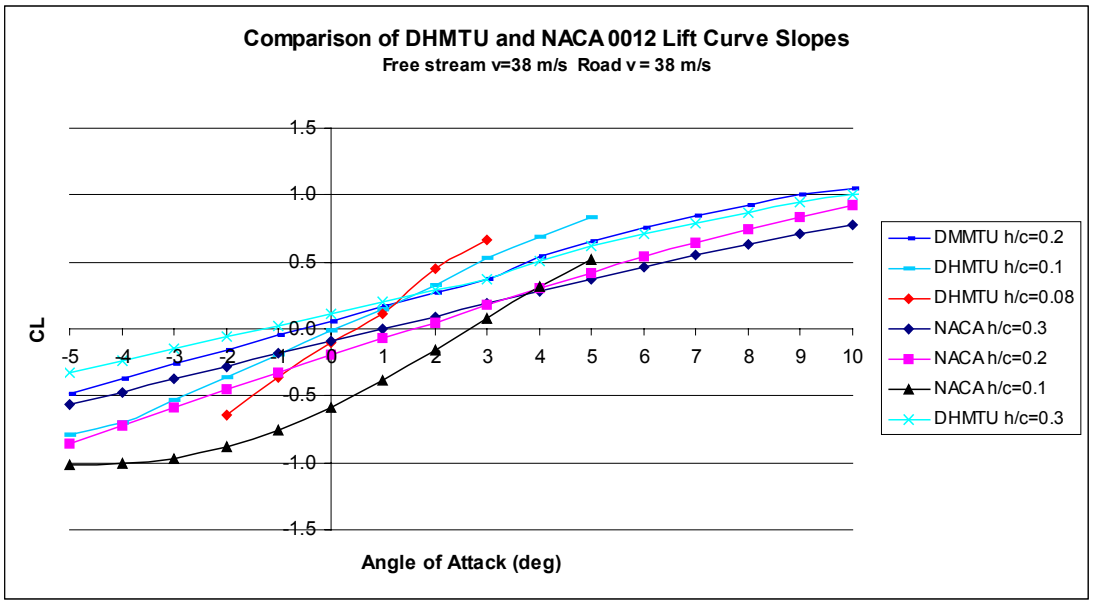

Figure 8: Comparison of DHMTU and NACA 0012 Lift Curve Slopes

One of the requirements for a ground effect section is for ∂CL/∂H to be a minimum (Table 1). Figures 9 and 10 illustrate the variation in C_L with altitude for the DHMTU and NACA 0012. In extreme ground effect the NACA 0012 produces a reduction of lift with decreasing altitude. The magnitude of the ∂CL/∂H for the NACA 0012 becomes more negative with decreasing angle of attack. At AoA of 1 degree C_L decreases by a factor of 5.3 between h/c 0.2 to 0.1. At AoA of 4 and 5 degrees the ram ground effect produces an increase in C_L. The DHMTU produces a negative gradient only at AoA 1 degree. As the AoA increases ∂CL/∂H for the DHMTU increases in magnitude at the operating AoA C_L increases by 1.3 times between h/c 0.2 to 0.1.

Angle of Attack (degrees)	NACA 0012 $\frac{\partial C_L}{\partial H}$	DHMTU $\frac{\partial C_L}{\partial H}$
1	-3.10	-0.20
2	-2.04	0.58
3	-1.01	1.56
4	-0.74	1.47
5	-0.28	1.77
6	0.12	N/O

Table 9: Variation of ∂CL/∂H in extreme ground effect

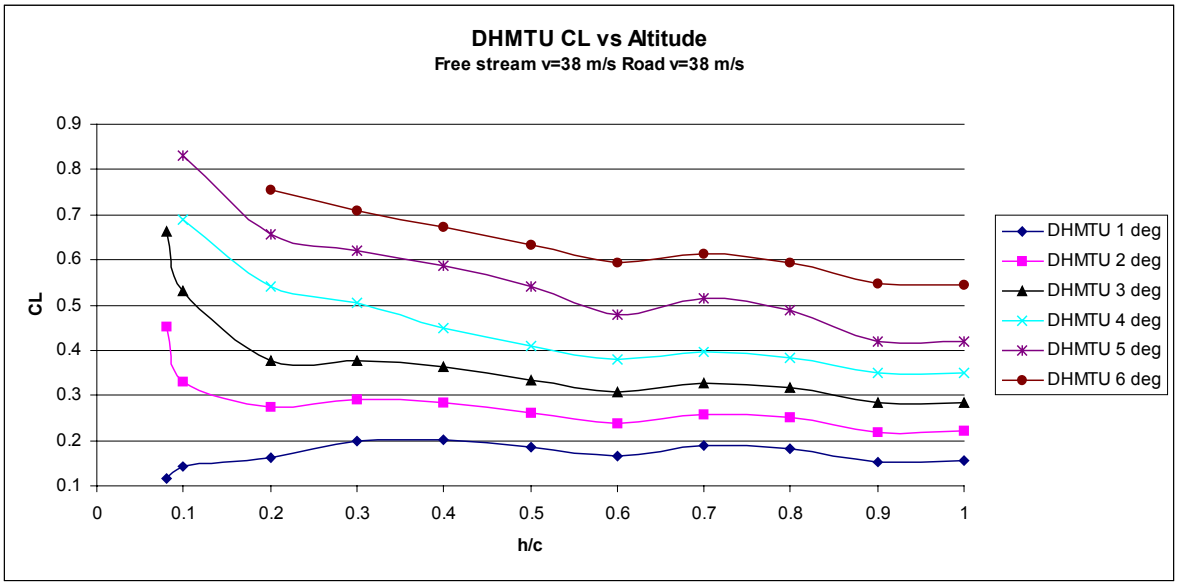

Figure 9: Variation of CL with altitude for DHMTU

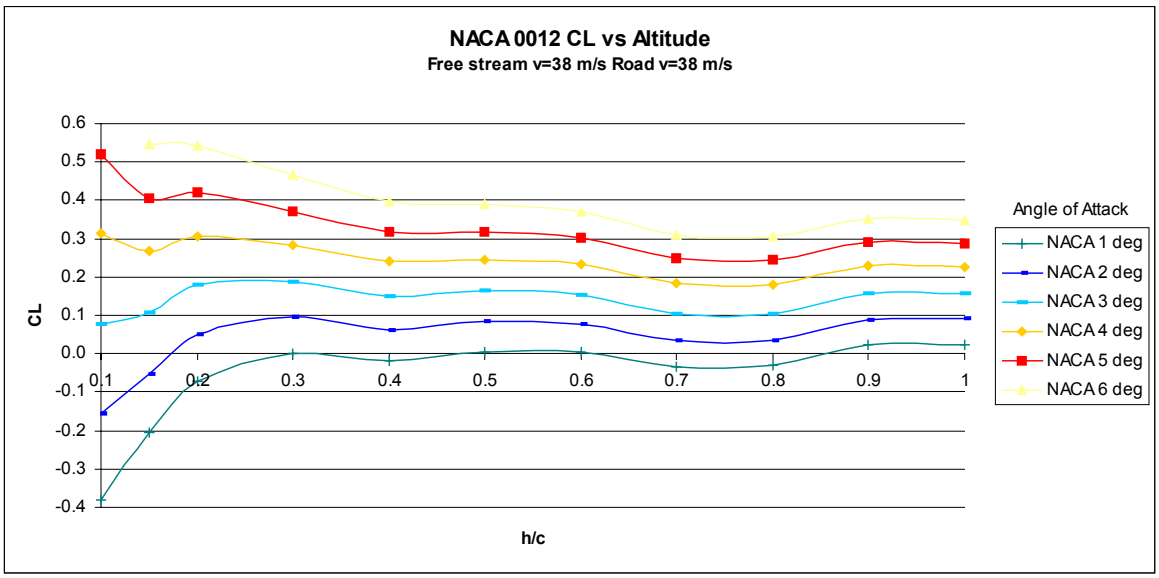

Figure 10: Variation of CL with altitude for NACA 0012

Within the range of Reynolds Numbers that runs were conducted no discernible effects on lift could be quantified (Figure 11).

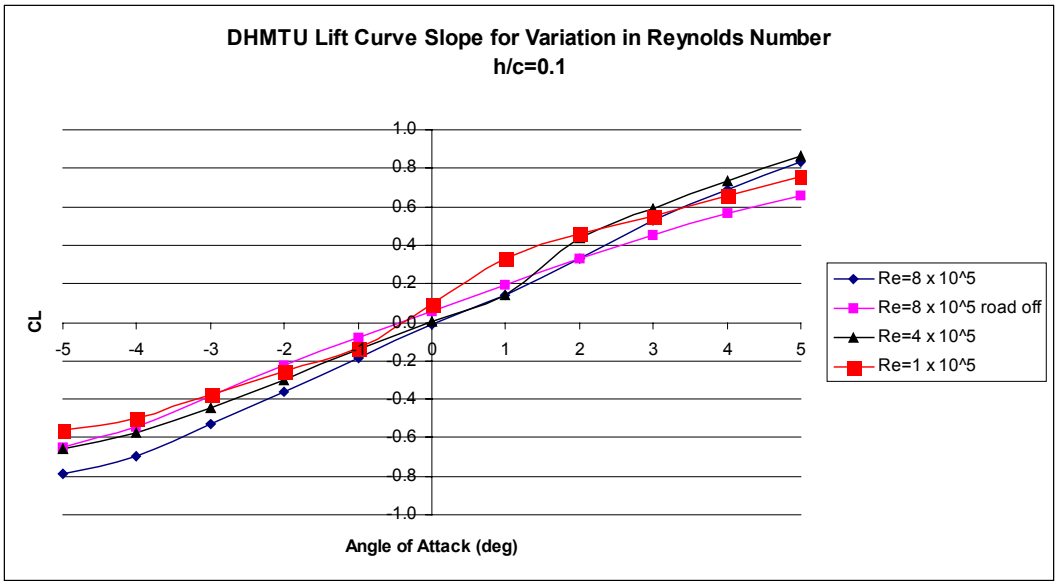

Figure 11: Effect of Reynolds Number variation on DHMTU lift characteristics

The maximum aerodynamic efficiency of the DHMTU section is achieved at an angle of attack of 5 degrees (Figure 12). At this optimum angle L/D ratios of upto 22 can be achieved at h/c below 0.1. It is possible that even greater values of aerodynamic efficiency could be produced at lower altitudes, if a reasonable range of AoA could be realised. Though this is constrained by the safe operating altitude of the wing.

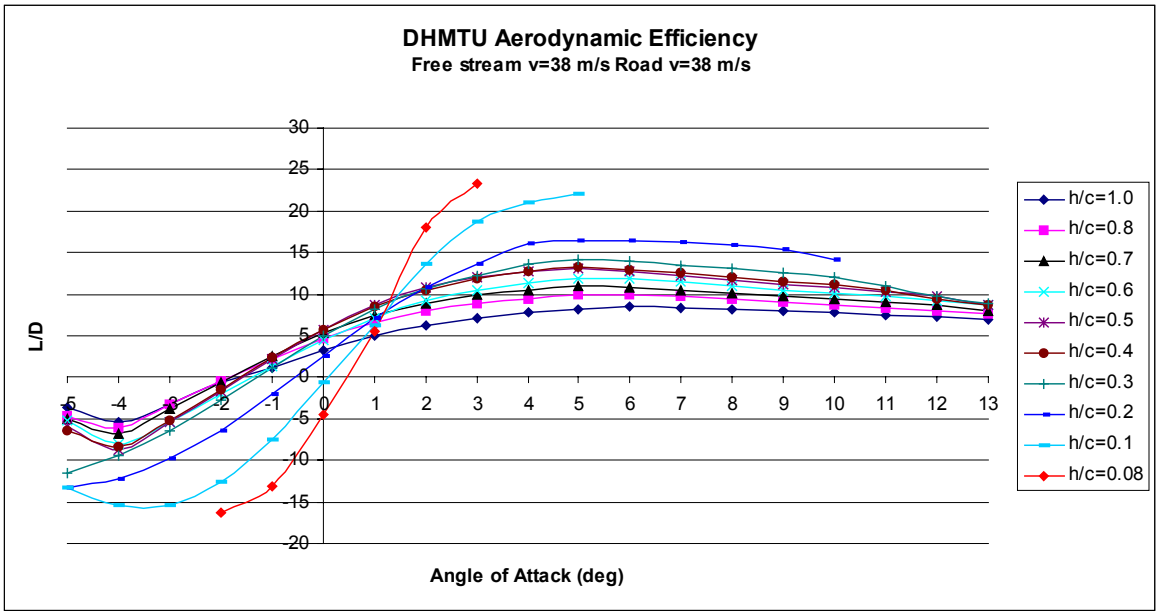

Figure 12: DMTU Aerodynamic Efficiency

The NACA 0012 produces peak L/D in excess of the DHMTU at h/c=0.2 and 0.3 and comparable at 0.1 (Table 10). This however is not the only measure of performance of the sections as an inspection of Figure 13 reveals. The efficiency curves of the NACA 0012 show that they provide greatly reduced performance at small angles of attack. At h/c=0.1 the NACA 0012 L/D provides no usable performance below AoA of 2.5 degrees. This also occurs at h/c=0.2 where below AoA of 1.5 degrees the NACA 0012 possesses no performance. Slight changes in AoA for NACA 0012 will result in radically different performance.

h/c	DHMTU L/D	AoA (degrees)	NACA 0012 L/D	AoA (degrees)
1	8.4	6	12.9	5
0.9	9.2	6	12.0	6
0.8	10.0	5	12.3	6

0.7	11.0	5	15.1	5
0.6	11.9	5	13.8	6
0.5	12.7	6	13.9	5
0.4	12.8	6	14.3	6
0.3	14.1	5	18.7	5
0.2	16.5	6	18.4	7
0.1	22.0	5	21.5	5

Table 10: Comparison of peak L/D for DHMTU and NACA 0012 Sections

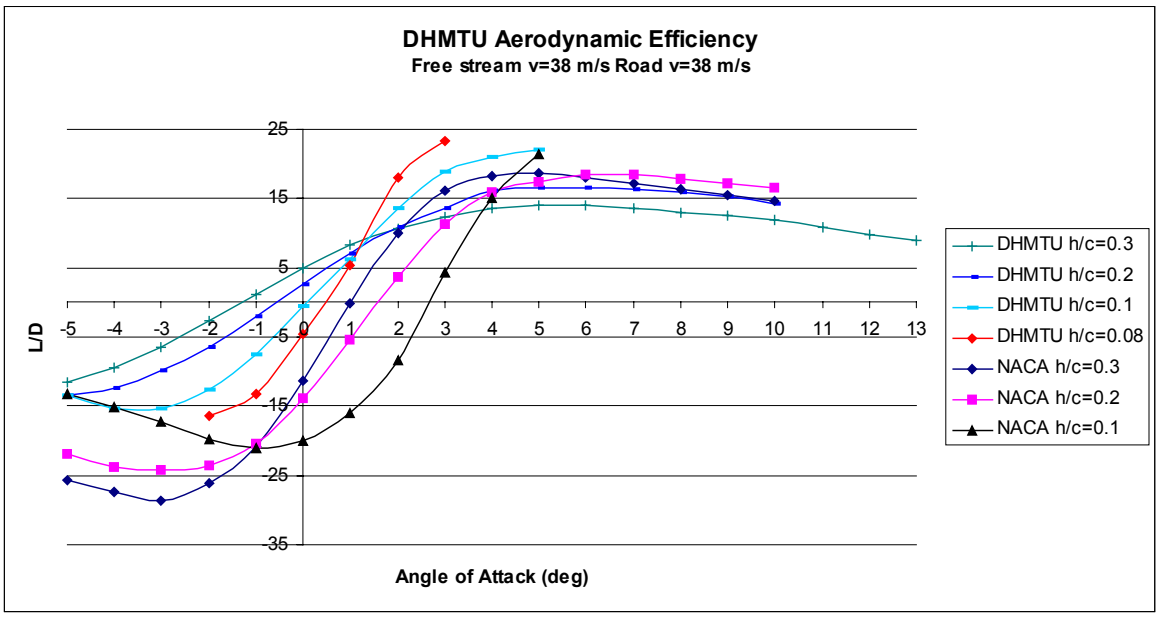

Figure 13: Comparison of DHMTU and NACA 0012 Aerodynamic Efficiencies

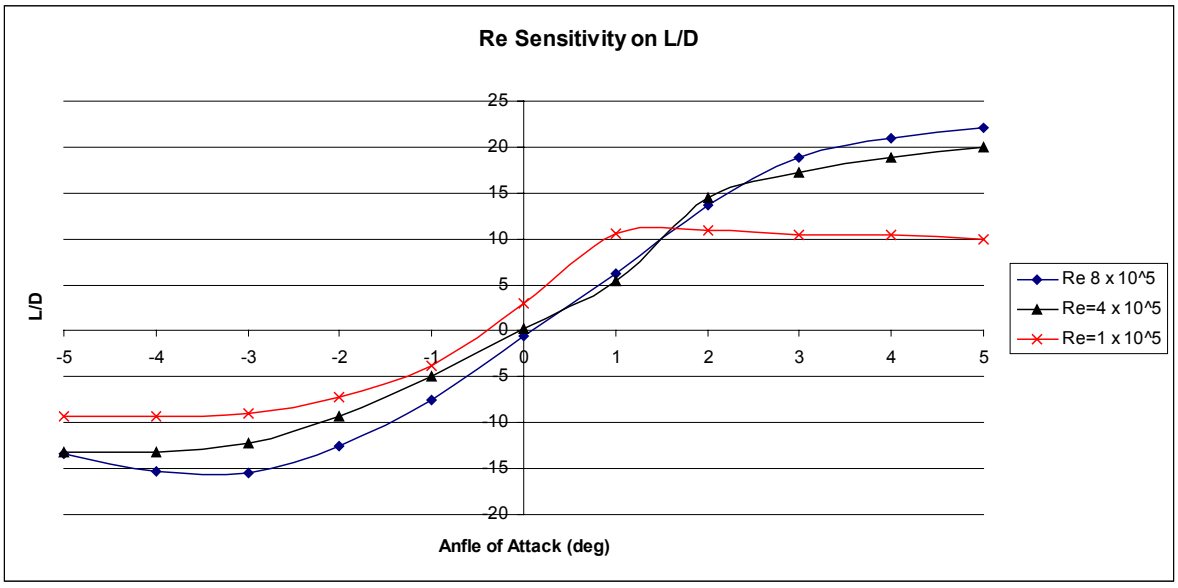

Figure 14: Effect of Reynolds Number on Aerodynamic Efficiency

At the low Reynolds Number aerodynamic efficiency is reduced from 22 at Re 8 x 10^5 to 10.5 at Re 1x10^5 (Figure 14). This is a result of the rapid increase in drag at AoA 1 degree as illustrated in Figure 6.

Figure 15 illustrates the pitch behaviour of the DHMTU section. One interesting feature that this graph illustrates is that the curve exhibits negative gradient and then a positive step indicating a region of reduced stability. The position that this change in behaviour occurs corresponds to the step change in lift (Table 6). Figure 16 graphically illustrates this correlation for h/c 0.1 to 0.3. The position of this region of relative instability decreases with reduced altitude and for altitudes between h/c=1 to 0.1 lies within AoA 5 to 1 degrees. This region of instability lies just below the optimum operating AoA of 5 to 6 degrees.

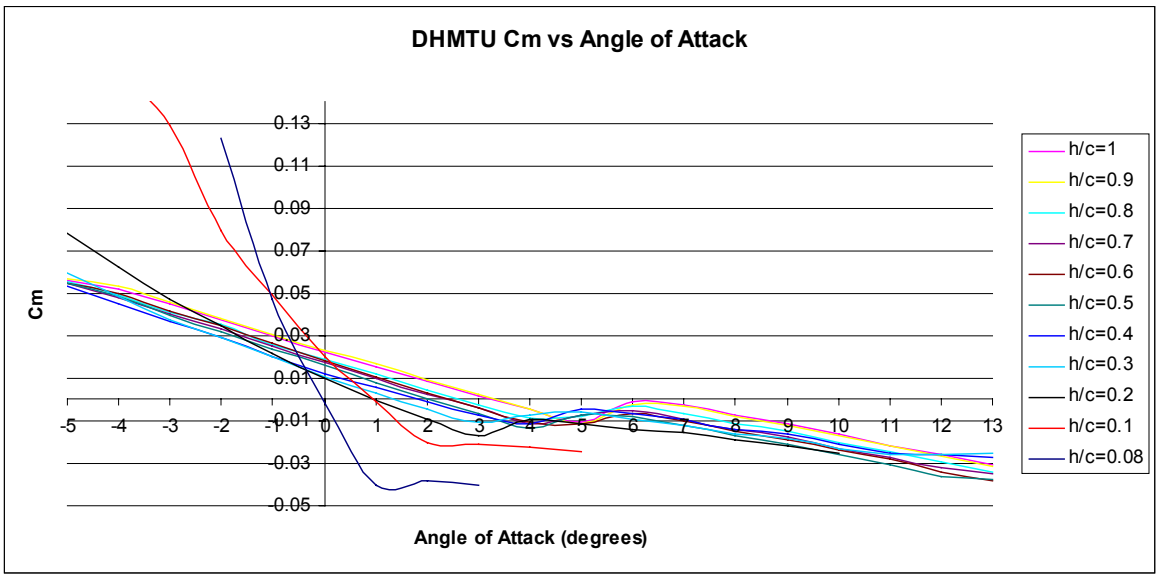

Figure 15: DHMTU Pitching Moment Response

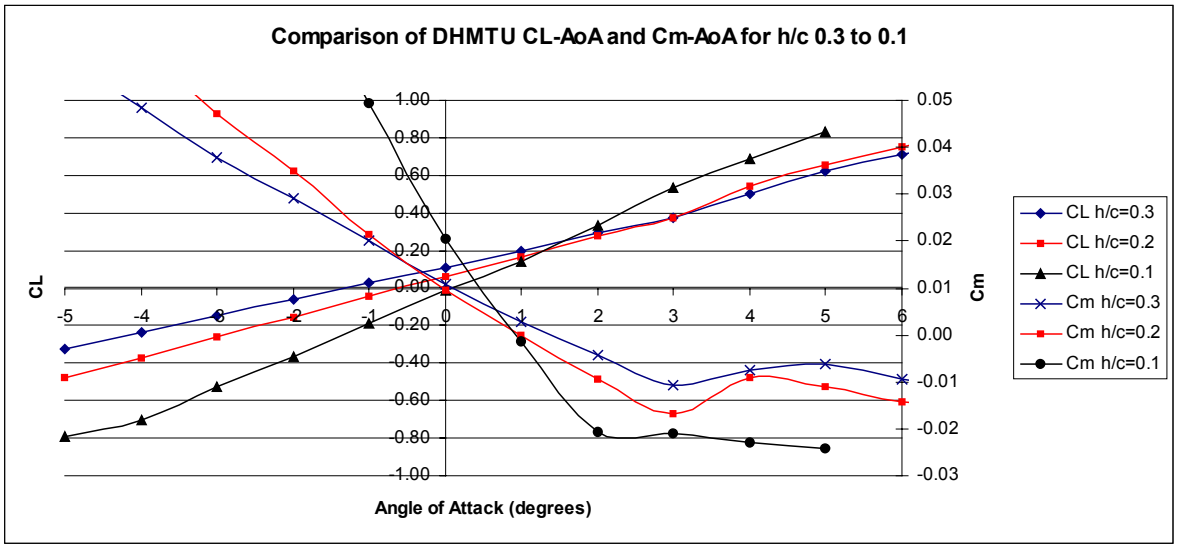

Figure 16: Comparison of Lift and Pitching Moment Curves for DHMTU h/c 0.1 to 0.3

Figure 17 illustrates the pitching behaviour of both sections in ground effect between h/c 1.0 to 0.5. As the altitude is decreased the respective behaviour of the NACA 0012 and DHMTU curves do not radically alter. The NACA 0012 exhibits linear behaviour upto 6 degrees AoA, whilst the DHMTU exhibits the characteristics step change in gradient as discussed above. The NACA 0012 develops a greater magnitude of downward pitching moment then the DHMTU section. This is presented in Table 11 where it can be seen as the altitude decreases from h/c 1 to h/c 0.5 the NACA 0012 produces from 2.1 to 7.1 times the Cm as the DHMTU. It can be seen from Table 12 that the DHMTU section posses a higher $dCm/d\alpha$ then the NACA 0012. This would result in the DHMTU providing a higher change in restoring pitching rate the NACA 0012.

h/c	NACA Cm/DHMTU Cm
1	2.15
0.9	2.14
0.8	3.00
0.7	3.58
0.6	2.61

0.5	4.16
0.4	7.09
0.3	5.61
0.2	4.37
0.1	4.02

Table 11: Ratio of NACA 0012 and DHMTU Cm at AoA 5 degrees

h/c	NACA 0012 $\frac{dC_m}{d\alpha}$	DHMTU $\frac{dC_m}{d\alpha}$
1	-0.0053	-0.0071
0.9	-0.0054	-0.0072
0.8	-0.0055	-0.0073
0.7	-0.0055	-0.0074
0.6	-0.0056	-0.0076
0.5	-0.0056	-0.0077
0.4	-0.0057	-0.0076
0.3	-0.0059	-0.0085
0.2	N/O	-0.0119
0.1	N/O	N/O

Table 12: Comparison of Cm-AoA gradient of NACA 0012 and DHMTU in linear region
* N/O Not Obtainable

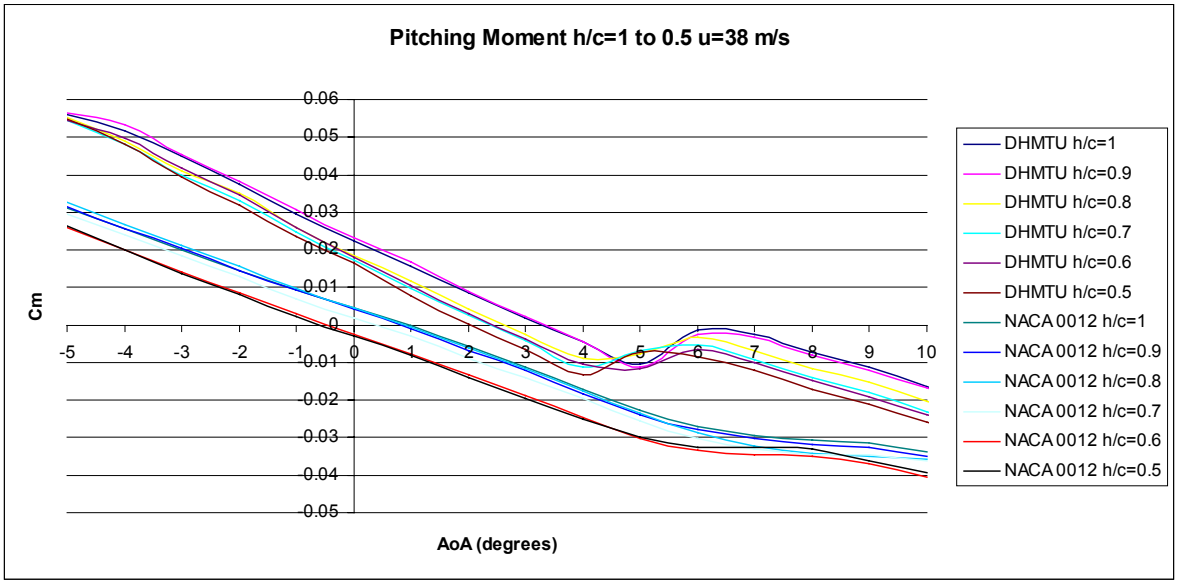

Figure 17: Pitch behaviour of NACA 0012 and DHMTU (upper set of lines) sections h/c=1 to 0.5

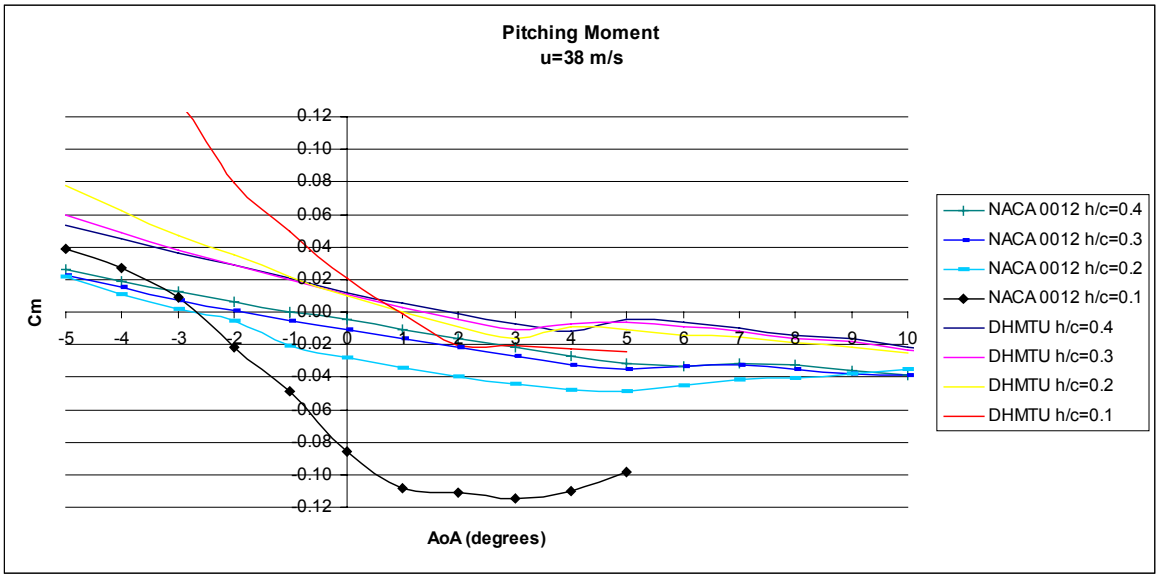

Figure 18: Pitch behaviour of NACA 0012 and DHMTU sections h/c=0.4 to 0.1

It can be seen from Figure 19 that the DHMTU section possesses a more linear pitching moment behaviour then the NACA 0012 with decreasing altitude.

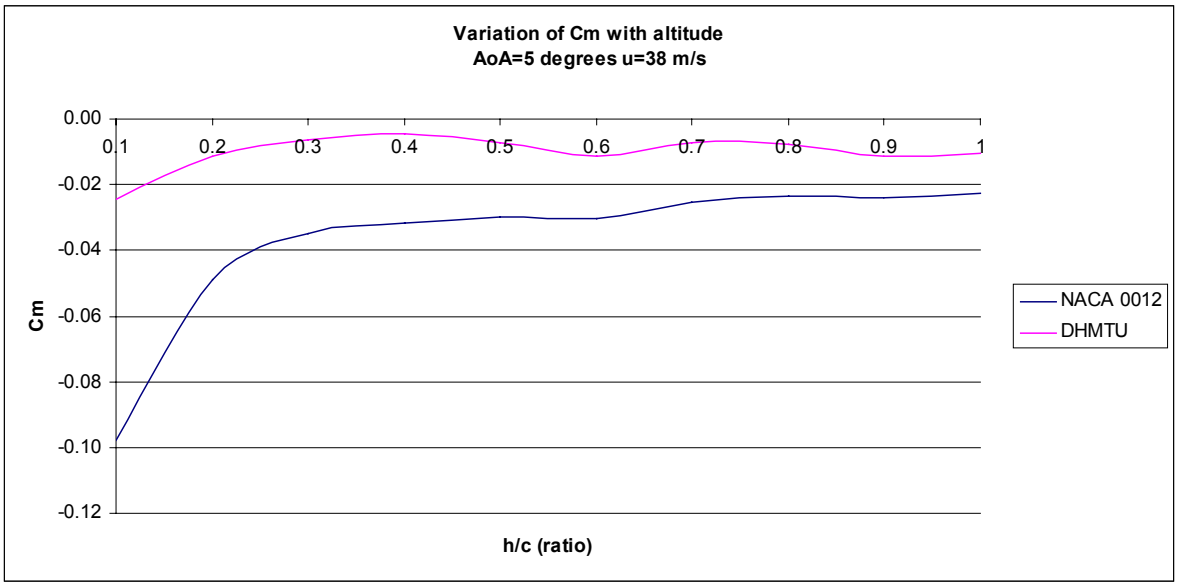

Figure 19: Variation with pitch behaviour as a function of altitude

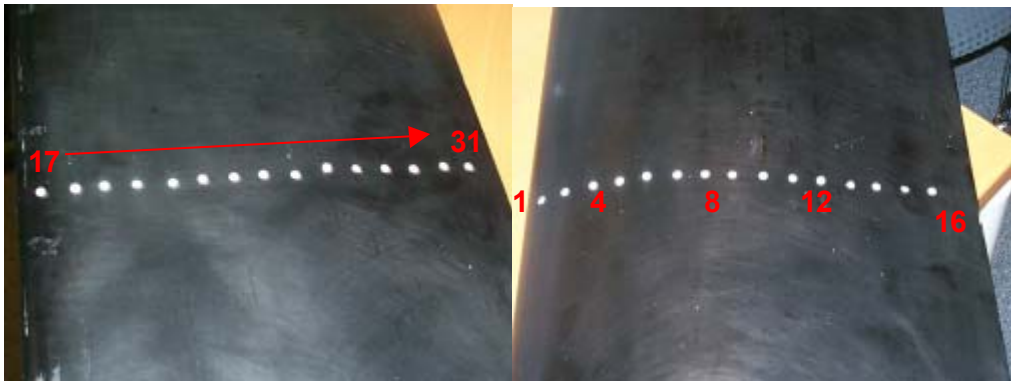

Figure 20: Location of Pressure Tappings on the DHMTU Lower (left) and Upper (right) surface

In order to investigate the pressure distribution around the DHMTU a total of 31 pressure tappings were made down the centre of the sections span. Figure 20 illustrates the location and the number assigned to each tapping. Figure 21 presents the behaviour of pressure along the underside of the DHMTU section as a function of altitude. The data is presented for an angle of attack of 3 degrees as this was the maximum that could be achieved at altitudes down to h/c=0.08.

The pressure tapping results provide further confirmation of the difference between moderate and extreme (h/c<0.1) ground effect. It is noticeable that when h/c falls below 0.2 the pressure under the section greatly increases. The rate at which the pressure increases is particularly evident when h/c<0.1 compared to the near linear nature of the pressure increase above an altitude of h/c=0.2. Here the pressure gradient across the lower section profile shows a rapid increase up to tapping 24, corresponding to a distance of 0.5c from the section leading edge.

As the altitude increases above h/c=0.2 a drop in pressure occurs at the trailing edge as the compressed airflow between the section and the ground diffuses. This is seen in the drastic drop of pressure at stations 30-31. These are located where the undersurface of the section reflexes upward (Figure 20).

As the altitude increases above h/c=0.6 suction is present on the undersurface from station 17 to 19. As the altitude decreases Cp increases due to the presence of the ground. Note that at h/c=0.08 there is a large reduction in pressure at station 17.

Figure 22 provides a graphical depiction of the airflow at h/c=0.15 and AoA 5 degrees. The spanwise component of the flow due to wingtip circulation is very evident. The flow separation at the trailing edge can be clearly discerned.

A major finding of interest is the large differences in pressure coefficient with small changes in altitude between h/c 0.08 and 0.3. If we consider a WIG with a chord of 10 m, translation in altitude of just 1 m in this altitude regime will produce a significant variation in the lift characteristics of the wing. This will require the vehicles control system to be able to provide rapid stabilising responses.

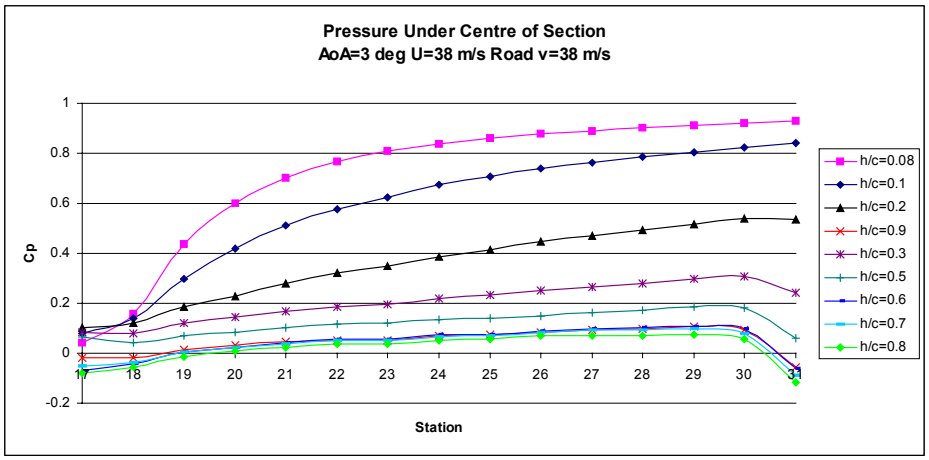

Figure 21: Pressure distribution under mid span of DHMTU

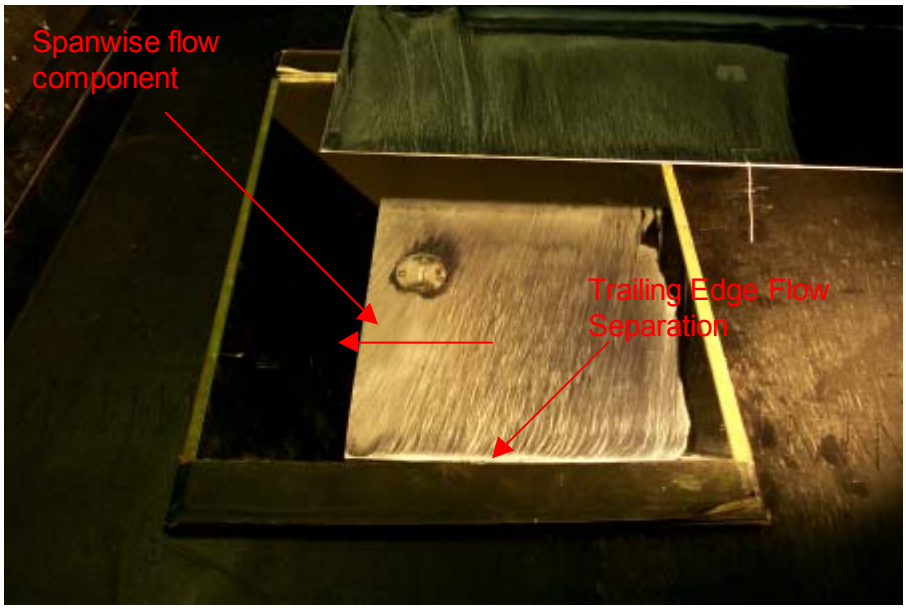

Figure 22: Underside of DHMTU illustrating trailing edge flow separation and spanwise flow direction due to wing tip circulation

The trends in the flow over the upper surface of the DHMTU can be seen in Figure 23. Increasing suction can be seen to occur between stations 1-2 as the flow accelerates over the sections nose. The suction remains relatively constant and high between stations 2 to 5 over increasing section camber. A reduction in suction is produced between stations 5-7 (1/3c from the leading edge) as the flow has separated. This separation can be seen in Figure 24 where the flow visualisation mixture has pooled. As the flow reattaches suction is maintained upto station 9 where a rapid increase in pressure occurs followed by a more gradual increase in pressure until station 16 near the trailing edge. The increase in suction with decreasing altitude is readily apparent. The greatest changes with altitude occur over the first half of the section upto station 9. The pressure distribution reveals that IGE the most scope for increasing the suction and thereby performance over the upper surface is by optimising the front half of the section. This includes parameters such as the leading edge nose radius and camber of the front of the section.

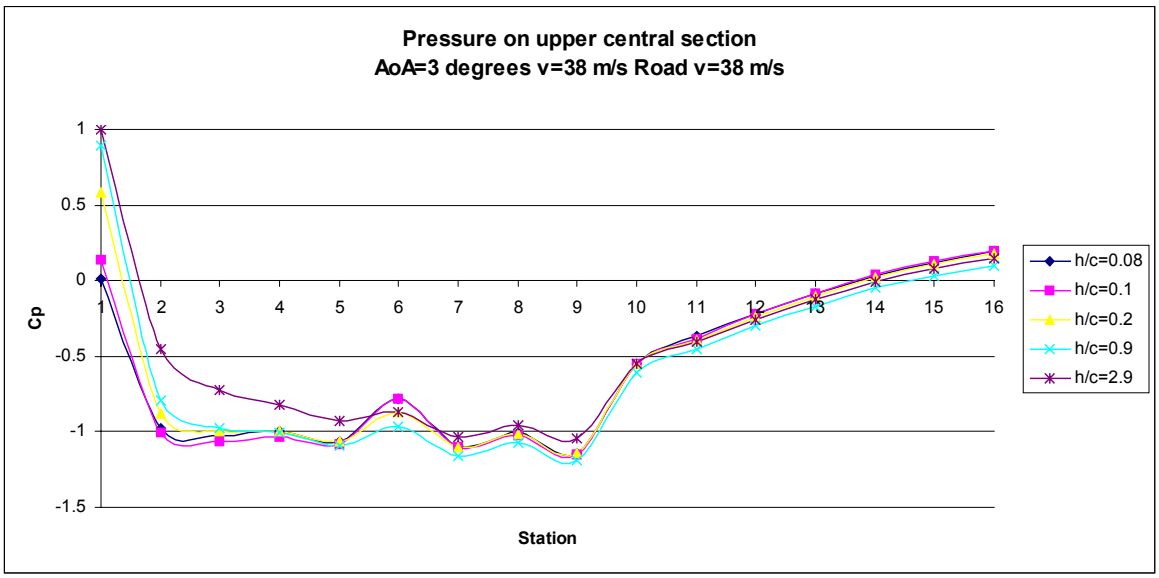

Figure 23: Pressure profile over upper DHMTU section

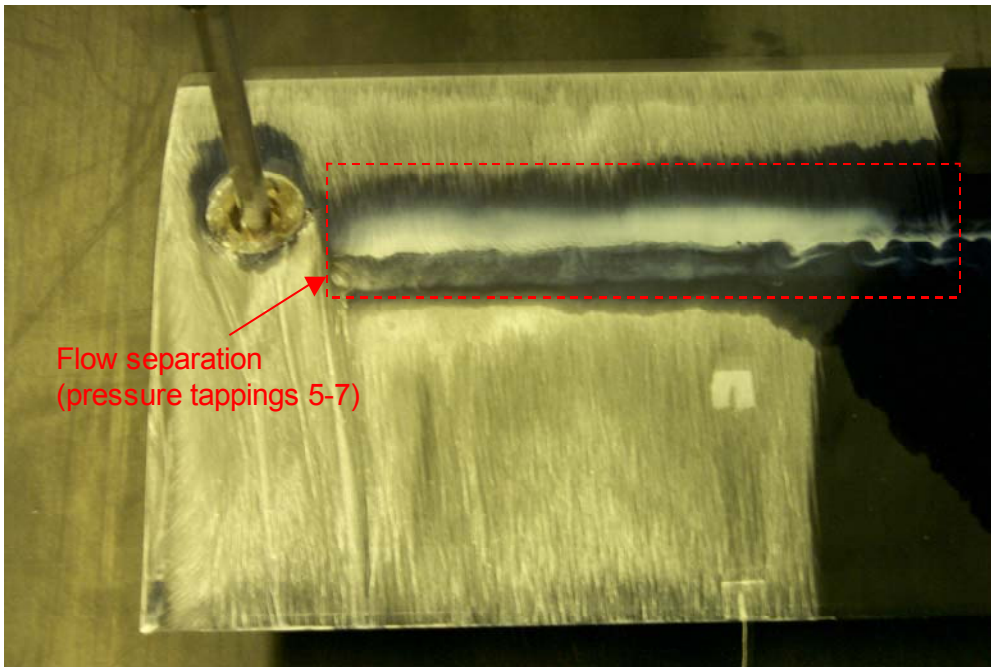

Figure 24: Flow over the top of DHMTU h/c=0.15 AoA=5 degrees

Conclusions

The research conducted so far has produced a large database of experimental data on a DHMTU 12-35.3-10.2-80.12 operating in the ground effect regime. It has been found that the overall drag of the DHMTU decreases with altitude contrary to discussions in the literature and the performance of the baseline NACA 0012. The drawback of the DHMTU variant tested is that it possesses higher drag characteristics then the NACA 0012 producing between 1.3 to 2.9 times the drag. The DHMTU lift curve slope exhibits an unusual distinctive step between AoA of 1 to 5 degrees depending on altitude. The DHMTU possesses superior lift generating performance between h/c 1 to 0.1 over the NACA 0012.

The NACA 0012 produces peak aerodynamic efficiencies in excess of the DHMTU at h/c=0.2 and 0.3 and comparable at 0.1. This however is not the only measure of performance of the sections, as the DHMTU produces superior performance at small angles of attack. Compared to the NACA 0012 control section the DHMTU possesses more consistent Cm behaviour with decreasing altitude. The DHMTU possesses a step in its Cm-AoA curve that indicates a region of relative instability between 1 to 5 degrees depending on altitude. This region lies just below the operating AoA regime (5-6 degrees) for maximum aerodynamic efficiency.

A major finding of interest is the large differences in pressure coefficient on the DHMTU's lower surface with small changes in altitude between h/c 0.08 and 0.3 resulting in significant variations in the lift characteristics of the wing and hence the control requirements from the vehicle itself. The upper surface pressure distribution reveals that for IGE the most scope for increasing the suction and thereby performance is by optimising the front half of the section of the wing.

References

1. Husa B, "WIG Configuration Development from Component Matrix", Orion Technologies, 05/08/00

2. Bolts C B, Clayton B R, “A Possible Maritime Future for Surface Effect Craft in the UK”, Symposium Proceedings of RAM Wing and Ground Effect Craft, Royal Aeronautical Society, 19th May 1987
3. Lange R, Moore J, “Large Wing-in-Ground Effect Transport Aircraft”, Journal of Aircraft, Vol.17, No.4, April 1980
4. Ollila R, “Historical Review of WIG Vehicles”, Journal of Hydronautics, Vol 14, No.3, July 1980
5. http://www.sea-technology.com
6. http://www.foster-marine.com/WIGCRAFT/web.pusan.ackr%20(DHMTU)/minggu.dir/~minggu/main.html
7. Tothill G M, “Flow Problems of WIGs/Ekranoplanes”, Part 3 Project, University of Southampton, 2001